ARTICLE

Check for updates

Journal of
Sensor Science and Technology

The Korean Sensors Society

Single-Layer SWIR Photodetector with a PbS Quantum Dot–Polymer Composite

Jinbeom Kwon[1,+]

[1]*Department of Semiconductor Engineering, Kyungwoon University, 730, Gangdong-ro, Sandong-eup, Gumi-si, Gyeongsangbuk-do 39160, Republic of Korea*

Cite This: *J. Sens. Sci. Technol. Vol. 34, No. 6 (2025) 618-622*

https://doi.org/10.46670/JSST.2025.34.6.618

ABSTRACT: With the rapid expansion of autonomous driving and smart-factory technologies, the demand for LIDAR sensors continues to increase. A short-wave infrared (SWIR) photodetector capable of detecting laser light for LIDAR 3D mapping is a key component of these systems. Among candidate materials, PbS quantum dots (QDs) enable low-cost, solution-processed fabrication and wavelength tunability within the eye-safe region above 1400 nm. However, conventional multilayer device structures require sequential solution deposition of electron and hole transport layers, which can cause interlayer dissolution and limit device stability. In this study, PbS QDs were synthesized with a target wavelength of 1533 nm and blended with [6,6]-phenyl-C61-butyric acid methyl ester (PCBM) and poly(3-hexylthiophene) (P3HT) to form a single composite ink. A monolithic SWIR photodetector was then fabricated via screen printing. The single-layer architecture enhanced carrier mobility and minimized interfacial defects. Structural and optical analyses confirmed the successful formation of PbS QDs, and electrical characterization under infrared illumination revealed a maximum photoresponse of 277%, a current change of approximately 440 μA, and a response time of 0.42 s. These results demonstrate that the PbS QD–PCBM–P3HT composite enables a simplified, stable, and high-performance SWIR photodetector suitable for next-generation LIDAR applications.

KEYWORDS: *Quantum dots, PbS QDs, SWIR, Photodetector*

1. INTRODUCTION

With the rapid advancement of automation technologies for future automobiles and smart factories, the demand for LiDAR sensors has increased sharply. LiDAR sensors scan the surrounding environment in real time to generate three-dimensional maps and accurately detect objects such as vehicles, pedestrians, and machinery, making them a core technology for autonomous systems [1,2]. A LiDAR sensor is composed of an infrared (IR) light source and an IR photodetector, among which the IR photodetector plays a critical role by detecting the IR light reflected from objects to enable 3D mapping. In particular, the performance of the IR photodetector determines the overall capability of the LiDAR system, as it must reliably sense IR signals even under adverse weather conditions or at night. Commercial LiDAR sensors currently rely primarily on indium gallium arsenide (InGaAs)-based near-infrared (NIR, 700–1000 nm) photodetectors [3,4]. While these devices exhibit high sensitivity and excellent stability, they require complex fabrication processes based on silicon and III–V compound epitaxial growth. This results in high manufacturing costs. Moreover, their operation at room temperature generates significant thermal noise, necessitating additional cooling systems. The NIR wavelength range also poses a safety concern, as it can penetrate the human retina and potentially cause damage.

To overcome these limitations, extensive research has focused on short-wave infrared (SWIR, 1000–2500 nm) photodetectors [5,6]. SWIR light provides higher transmittance and lower scattering than NIR, delivering superior image resolution in nighttime or harsh weather environments. In particular, the 1400–2500 nm range is classified as eye-safe because it cannot penetrate the human retina. Among the various SWIR photodetector technologies, quantum-dots (QDs)-based devices have attracted considerable interest [7]. Lead sulfide (PbS) QDs are particularly promising because they can be synthesized and processed via solution

[+]Corresponding author: jinbum0301@ikw.ac.kr
Received : Oct. 10, 2025, Revised : Oct. 19, 2025, Accepted : Oct. 23, 2025

methods, enabling low-cost and straightforward device fabrication. In addition, their bandgap can be tuned by controlling particle size, enabling detection across the 1000–2800 nm wavelength range and making them ideal for eye-safe photodetectors. However, high-performance devices typically require the deposition of electron and hole transport layers [8]. When these layers are stacked using solution processes, interlayer dissolution can occur, compromising film integrity. Therefore, simplified device architectures that minimize multilayer deposition while maintaining high sensitivity and structural stability are urgently required.

In this study, PbS QDs with a target absorption at 1533 nm were synthesized, and a composite ink was prepared by blending PbS QDs with [6,6]-phenyl-C61-butyric acid methyl ester (PCBM) as the electron-transport material and poly(3-hexylthiophene) (P3HT) as the hole-transport material. With this composite ink, a single-layer SWIR photodetector was fabricated via screen printing. The resulting monolayer enhances both electron and hole mobility, thereby achieving high sensitivity and fast response. The structural and optical properties of the synthesized PbS QDs were characterized by absorption spectroscopy and X-ray diffraction (XRD). The electrical performance of the fabricated device was evaluated using a source meter unit (SMU) under IR illumination. The optimized single-layer SWIR photodetector exhibited a maximum sensitivity of 120%, a current change of approximately 10 μA, and a response time of 0.4 s.

2. EXPERIMENTAL

2.1 Synthesis of PbS Quantum Dots

PbS QDs were synthesized using a colloidal method [11]. First, a sulfur precursor solution was prepared by dispersing 1 mmol of sulfur powder (S) in 2.4 mL of oleylamine (OLA) and stirring the mixture at room temperature for 30 min under a nitrogen atmosphere. Separately, a lead precursor solution was prepared by dissolving 1.5 mmol of lead(II) chloride ($PbCl_2$) in 5 mL of OLA and stirring under nitrogen for 30 min at room temperature, followed by heating to 160°C for 1 h. To remove residual impurities, we degassed the lead precursor solution under a vacuum at 120°C for 15 min. The reaction temperature was then adjusted to 110°C, and 225 μL of the S–OLA solution together with 274 μL of trioctylphosphine (TOP) were swiftly injected into the $PbCl_2$–OLA solution under a nitrogen flow. After 30 min of reaction, the mixture was cooled to room temperature. The resulting product was washed by adding methanol and toluene to the crude solution in a 4:1:1 ratio, followed by centrifugation at 3000 rpm for 5 min to isolate the PbS QDs. Finally, the purified QDs were redispersed in toluene to obtain a PbS colloidal solution with a concentration of 20 mg/mL^{-1}.

Table 1. Mixing ratios of PbS quantum dots and electron/hole extraction layers.

Material	Sample 1	Sample 2	Sample 3	Sample 4
PbS QDs (mg)	20	20	20	20
PCBM (mg)	20	10	5	0
P3HT (mg)	20	10	5	0
Ethyl cellulose (mg)	10	10	10	10
Toluene (mL)	1	1	1	1

2.2 Synthesis of PbS Quantum Dot Composite paste

The PbS QD composite paste was prepared using conductive polymers as charge-transport materials. PCBM was employed as the electron-transport layer and P3HT as the hole-transport layer [15,19]. PbS QD solution (1 mL) dispersed in toluene at a concentration of 20 mg/mL^{-1} was mixed with PCBM and P3HT at various ratios, as summarized in Table 1. The total amount of PCBM and P3HT was adjusted to be greater than, equal to, or less than the amount of PbS QDs to investigate the effect of composition. For comparison, an additional paste containing only PbS QDs without electron or hole transport layers was also prepared. To increase the viscosity required for screen-printing fabrication, we added 10 mg of ethyl cellulose as a rheology modifier. The mixture was stirred in air at 60°C for 3 h and then additionally stirred at room temperature for 12 h.

2.3 Fabrication of PbS Quantum Dot-Based SWIR Photodetector

The SWIR photodetector was fabricated using a screen-printing technique [19]. As the substrate, 5 mm × 5 mm alumina plates were sequentially cleaned with acetone, methanol, and isopropyl alcohol (IPA). Interdigitated (IDE) silver electrodes were then deposited onto the cleaned substrates by screen printing with silver paste. The prepared PbS QDs composite ink was subsequently printed through a shadow mask defining a 3 mm × 3 mm active area onto the silver IDE electrodes, according to the desired composition conditions. After printing, the devices were annealed at 95°C for 30 min to remove residual solvent, yielding photodetectors with a 9 mm^2 sensing region.

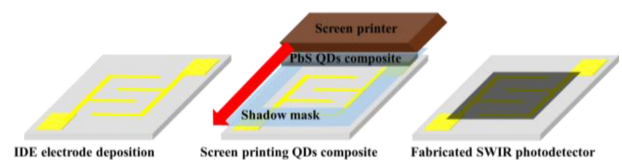

Fig. 1. Schematic diagram of the fabrication of a SWIR photodetector based on a PbS QDs composite.

3. RESULTS AND DISCUSSIONS

3.1 Characteristics of the synthesized PbS QDs

The characteristics of the synthesized PbS QDs were evaluated using absorbance spectroscopy and XRD. As shown in Fig. 2(a), the QDs exhibited a distinct absorption peak at 1533 nm with a full width at half maximum (FWHM) of 102 nm [5,6,17]. This narrow bandwidth confirms the ability of the QDs to selectively detect IR light in the 1533 nm region, which lies within the eye-safe range, and suggests that photodetectors based on these QDs can achieve high selectivity and excellent photo response.

For structural analysis, thin films were prepared by spin-coating a 20 mg mL^{-1} PbS QD solution onto 15 mm × 15 mm glass substrates at 1500 rpm for 30 s, followed by annealing at 95°C for 30 min. As shown in Fig. 2(b), the XRD pattern displayed diffraction peaks such as (111), (200), and (220) near 25.9°, 39.7°, and 42.8°, consistent with reported PbS crystal planes, confirming the successful synthesis of well-crystallized PbS QDs [11,17].

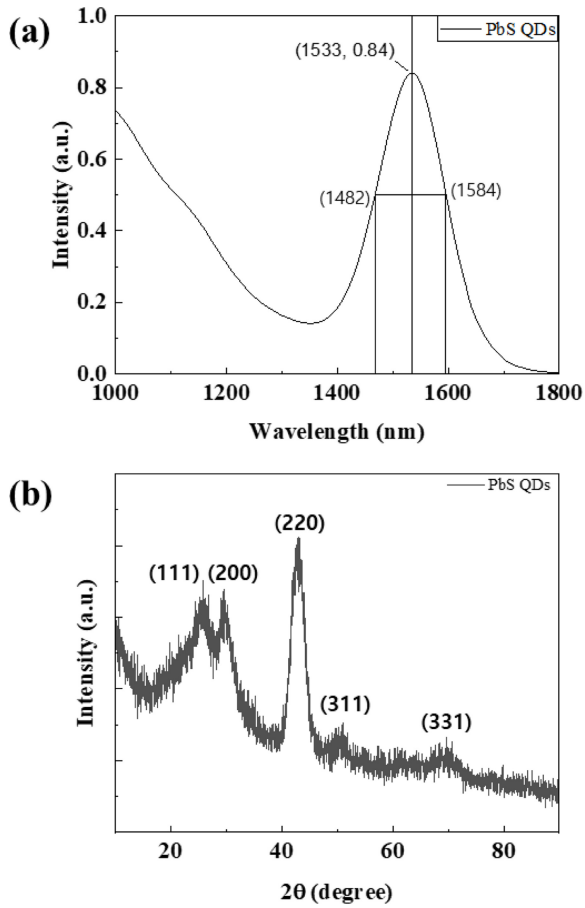

Fig. 2. (a) Absorbance and (b) XRD analysis characteristics of synthesized PbS QDs.

3.2 Characteristics of the fabricated SWIR photodetector

The electrical and photoresponse characteristics of the fabricated PbS QD-based SWIR photodetectors were evaluated in an optical chamber. Each device was mounted with probe tips, and measurements were performed using an SMU (B2902A, Keysight) under an applied bias of 3 V [12-15]. An IR light source (Thorlabs, SLS202L/M) provided illumination to compare current variations under illuminated and dark conditions. Three types of SWIR photodetectors were characterized under identical conditions, and both the light current (under IR illumination) and dark current (without illumination) were measured. As shown in Fig. 3, Sample 2, which was prepared with PCBM (10 mg) and P3HT (10 mg) in a total amount equal to that of the PbS QDs, exhibited the highest current change of approximately 440 μA. The graphs in Fig. 3(b) and 3(d) were enlarged to evaluate the response and recovery times, and the times required to reach 90% of the total current increase after the light was turned on and 90% of the total current decrease after the light was turned off were calculated. Consequently, the response and recovery times were determined to be approximately 0.42 and 0.75 s, respectively. This result indicated that electrons and holes generated in the PbS QDs were efficiently extracted through PCBM and P3HT, which have high charge mobilities, producing large current modulation and a rapid photo response [20-22]. When the combined concentration of PCBM and P3HT exceeded that of the PbS QDs, the density of QDs in the active layer decreased, lowering the IR absorption efficiency. The reduced QDs density also promoted defect formation and localized oxidation, which introduced trap states and enhanced charge recombination, yielding a markedly smaller current change of only ~0.412 μA. Conversely, when the combined concentration of PCBM and P3HT was lower than that of the QDs, the charge mobility was insufficient, resulting in diminished current modulation and slower response [7,18,19]. A reference device composed exclusively of PbS QDs, without electron- and hole-transport layers, exhibited a current change of only ~0.35 μA, slow response, and high noise. This behavior is attributed to poor film uniformity and limited charge-transport pathways in the absence of the conductive polymers that enhance film adhesion and facilitate carrier extraction [6,11,13]. The photoresponse of each device was quantified as the percentage change in current relative to the dark current, calculated using equation (1) [12,14,22].

$$\text{Photoresponse (\%)} = \frac{I_{light} - I_{dark}}{I_{dark}} \times 100 \quad (1)$$

As presented in Fig. 5, the device of Sample 2 exhibited a photoresponse of 277%, approximately 27 times higher than

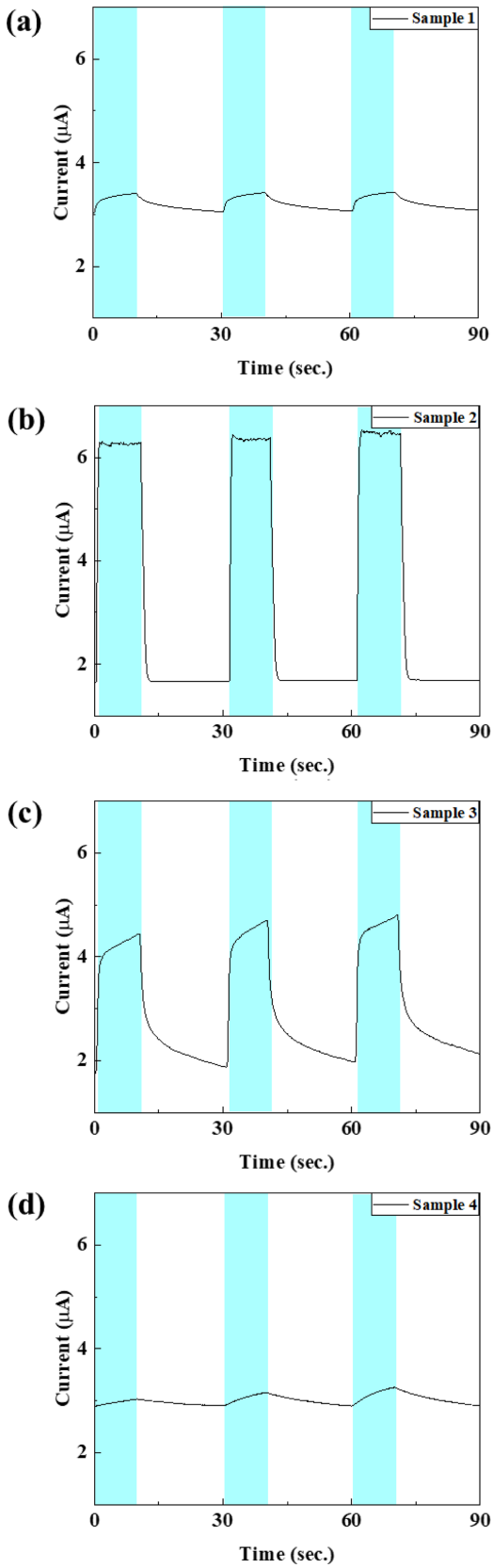

Fig. 3. Current characteristics of SWIR photodetectors under light source irradiation according to PbS QDs composite mixing conditions (a) Sample 1, (b) Sample 2, (c) Sample 3, and (d) Sample 4.

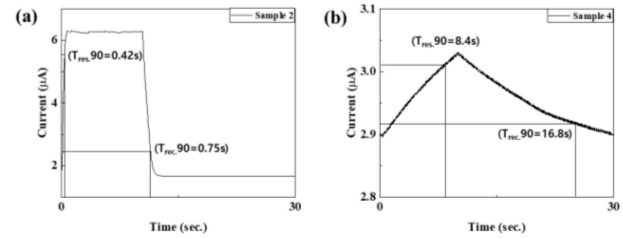

Fig. 4. Enlarged graphs of (a) Samples 2 and (b) Sample 4 for the calculation of response and recovery times.

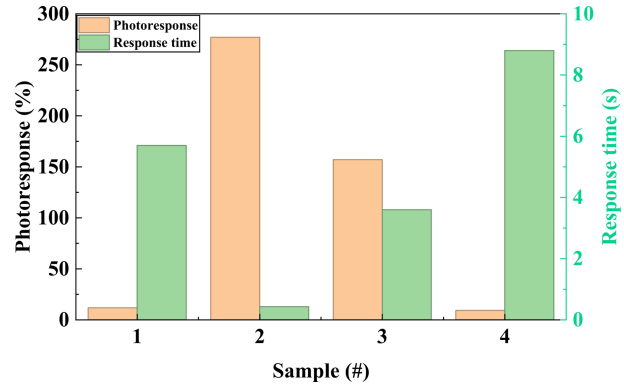

Fig. 5. Photoresponse and response time characteristics of the fabricated SWIR photodetectors.

that of Sample 4, which showed the lowest value. Furthermore, the response time of Sample 2 was about 20 times faster than that of Sample 4.

4. CONCLUSIONS

A high-performance short-wave infrared (SWIR) photodetector was developed using a fully solution-processed, screen-printing method based on a PbS QDs composite [15,19]. PbS QDs synthesized using a colloidal route exhibited a sharp absorption peak at 1533 nm with a 102 nm full width at half maximum, and XRD confirmed their high crystallinity and strong, eye-safe infrared absorption. To simplify the device architecture and improve charge transport, we blended the QDs with [6,6]-phenyl-C61-butyric acid methyl ester (PCBM) and poly(3-hexylthiophene) (P3HT) to form a single printable layer. A systematic variation of the PCBM/P3HT ratio revealed that a composition in which the combined amount of PCBM and P3HT equaled that of the PbS QDs provided the best performance. This device delivered a current change of about 10 μA, a photo response of roughly 277%, and a rapid response/recovery time of 0.43/0.75 s. Devices with either excess or insufficient polymer content exhibited reduced QDs density, trap formation, or limited carrier mobility, leading to markedly lower photo response, whereas a reference device

composed exclusively of PbS QDs exhibited the poorest characteristics. These findings demonstrate that a monolithic PbS QDs–PCBM–P3HT layer enables a simplified, stable, and low-cost SWIR photodetector, offering a practical and scalable route toward eye-safe infrared sensors for next-generation LiDAR and related optoelectronic applications.

CRediT Authorship Contribution Statement

Jinbeom Kwon : Carried out all aspects of the research and manuscript preparation.

Declaration of Competing Interest

The author declare that they have no known competing financial interests or personal relationships that could have appeared to influence the work reported in this paper.

Acknowledgements

This research received no external funding.

REFERENCES

[1] J.F. Klem, J.K. Kim, M.J. Cich, G.A. Keeler, S.D. Hawkins, T.R. Fortune, Mesa-isolated InGaAs photodetectors with low dark current, Appl. Phys. Lett. 95 (2009) 031112.
[2] J. Cao, Y. Yu, T. Li, C. Yu, Y. Gu, B. Yang, et al., Lightly doped $In_{0.53}Ga_{0.47}As$/InP SWIR photodetectors with diffusion barrier structure, Infrared Phys. Technol. 137 (2024) 105112.
[3] J. Zhang, W. Wang, H. Ye, R. Huang, C. Liu, W. Zhao, et al., Ultra-broadband ultraviolet–visible light–short wavelength infrared InGaAs focal plane arrays via n-InP contact layer removal, Sensors 24 (2024) 1521.
[4] R. Nagi, J. Bregman, G. Mizuno, P. Oduor, R. Olah, A.K. Dutta, et al., Development of high performance SWIR InGaAs focal plane array, Proceedings of the SPIE Defense, Security, and Sensing 2015, Baltimore, USA, 2015, p. 9481–05.
[5] J.B. Kwon, S.-W. Kim, B.-H. Kang, S.-H. Yeom, W.-H. Lee, D.-H. Kwon, et al., Air-stable and ultrasensitive solution-cast SWIR photodetectors utilizing modified core/shell colloidal quantum dots, Nano Converg. 7 (2020) 28.
[6] J.B. Kwon, S. Kim, J. Lee, C. Park, O. Kim, B. Xu, et al., Uncooled short-wave infrared sensor based on PbS quantum dots, Nanomaterials 9 (2019) 926.
[7] J.B. Kwon, M. Han, D.G. Jung, S.H. Kong, D. Jung, High sensitivity shortwave infrared photodetector based on PbS quantum dots and conductive polymer, Nanomaterials 11 (2021) 2683.
[8] J.B. Kwon, Y. Ha, S. Choi, D. Jung, Development of a highly reliable PbS QDs-based SWIR photodetector based on metal oxide electron/hole extraction layer formation conditions, Nanomaterials 15 (2025) 1107.
[9] J.B. Kwon, Y. Ha, S. Choi, D G. Jung, H.K. An, S.H. Kong, et al., Solution-processed NO_2 gas sensor based on poly(3-hexylthiophene)-doped PbS quantum dots operable at room temperature, Sci. Rep. 14 (2024) 20600.
[10] S. Choi, J.B. Kwon, Y. Ha, D. Jung, Short-wave infrared photodetector based on PbS quantum dots for eye-safe LiDAR sensors, J. Korean Phys. Soc. 83 (2023) 455–463.
[11] E. Heves, Y. Gurbuz, PbS colloidal quantum dot photodiodes for SWIR detection, Procedia Eng. 47 (2012) 1426–1429.
[12] H.C.V. Tran, E. Jang, J. Kim, M. Choi, Y. Park, H. Jeong, et al., Enhanced SWIR Photodetection in Colloidal Quantum Dot Photodiodes via Tunneling Current Suppression, ACS Appl. Mater. Interfaces 17 (2025) 15666–15674.
[13] F. Fang, Y. Tang, H. Tang, Y. Song, Q. Chen, L. Rao, et al., Interface-Enhanced PbS Quantum Dot Short-Wave Infrared Photodetector toward Instant Smoke Detection Applications, ACS Appl. Electron. Mater. 7 (2025) 7368–7376.
[14] M. Vafaie, J.Z. Fan, A.M. Najarian, O. Ouellette, L.K. Sagar, K. Bertens, et al., Colloidal quantum dot photodetectors with 10-ns response time and 80% quantum efficiency at 1,550 nm, Matter 4 (2021) 1042–1053.
[15] S. Chang, J. Jin, J. Kyhm, T.H. Park, J. Ahn, S.Y.L. Park, et al., SWIR imaging using PbS QD photodiode array sensors, Opt. Express 30 (2022) 20659–20665.
[16] S. Li, Z. Wang, B. Robertz, D. Neumaier, O. Txoperena, A. Maestre, A. Zurutuza, et al., Graphene–PbS QD hybrid photodetectors from 200 mm wafer-scale processing, Sci. Rep. 15 (2025) 14706.
[17] Q. Wang, C. You, Q. Yan, Q. Xie, W. Deng, M. Liu, et al., Size-controllable fabrication of PbS quantum dots for NIR–SWIR photodetectors with extended wavelengths, J. Mater. Chem. C 12 (2024) 19595–19602.
[18] M. Yang, H. Liu, S. Wen, Y. Du, F. Gao, Optimizing the infrared photoelectric detection performance of PbS quantum dots through solid-state ligand exchange, Materials 15 (2022) 9058.
[19] Y. Jiang, T. Ma, X. Gu, T. Jia, Y. Hong, Y. Huang, et al., Inkjet-printed PbS QD–graphene infrared photodetector with enhanced responsivity, Adv. Opt. Mater. 13 (2025) 00804.
[20] A. Vahl, J. Carstensen, S. Kaps, O. Lupan, T. Strunskus, R. Adelung, et al., Concept and modelling of memsensors as two terminal devices with enhanced capabilities in neuromorphic engineering, Sci. Rep. 9 (2019) 4361.
[21] L. Meng, T. Zeng, Y. Jin, Q. Xu, X. Wang, Surface-modified substrates for quantum dot inks in printed electronics, ACS Omega 4 (2019) 4161–4168.
[22] T. Jia, Y. Hong, Z. Wei, B. Mu, X. Yu, Two-step ligand-exchange-assisted charge transfer in graphene/PbS quantum dots hybrid near-infrared photodetector, ACS Appl. Electron. Mater. 6 (2024) 2066–2074.
[23] IEC 60825-1, Safety of laser products – Part 1: Equipment classification and requirements, Int. Electrotech. Comm. (2021).